iJRASET
International Journal For Research in Applied Science and Engineering Technology

INTERNATIONAL JOURNAL FOR RESEARCH

IN APPLIED SCIENCE & ENGINEERING TECHNOLOGY

Volume: 6 **Issue:** I **Month of publication:** January 2018

DOI: http://doi.org/10.22214/ijraset.2018.1294

www.ijraset.com

Call: 08813907089 | E-mail ID: ijraset@gmail.com

International Journal for Research in Applied Science & Engineering Technology (IJRASET)
ISSN: 2321-9653; IC Value: 45.98; SJ Impact Factor :6.887
Volume 6 Issue I, January 2018- Available at www.ijraset.com

Influence of Capping Agent on Structural and Optical Properties of Erium Oxide Nanoparticles Synthesized by Co-Precipitation and Green Method

Biju Joy[1]
[1]*Department of Chemistry, St. Xavier's College, Thumba Trivandrum, India.*

Abstract: ***The Monoethanolamine (MEA) capped cerium oxide Nanoparticles (CeO_2 NPs: B1) and Gloriosasuperba (G. superba) capped CeO_2 NPs (B2) were synthesized through co-precipitation and Green method. X-ray diffraction studies revealed that the synthesized MEA and G. superba capped CeO_2 NPs exhibited cubic phase. Morphological and elemental composition was studied FESEM and EDAX spectra. From the FTIR spectra, the Ce-O stretching band was observed at 505 and 508 cm^{-1} for MEA and G. superba capped CeO_2 NPs respectively. UV-Visible absorption spectra, the band gaps of MEA and G. superba capped CeO_2 NPs were calculated at 2.6 and 2.95 eV, respectively. The photoluminescence measurements revealed that the broad emissions were composed of five different peaks observed for MEA capped CeO_2 NPs.***
Keywords: Monoethanolamine; G. superba; capping agent; CeO_2; XRD; FESEM.

I. INTRODUCTION

Cerium oxide nanoparticles (CeO_2 NPs) are technological important material with desirable properties used wide applications, such as heterogeneous catalysts, high charge storage capacitors, corrosion-resistance materials, UV-protective coating and gas sensor materials [1-3]. In the literature, syntheses of nanoparticles have been achieved by various methods incorporated with physical and chemical way, such as hydrothermal, flame spray pyrolysis, sonochemical, microwave, sol-gel, and co-precipitation methods [4-9]. Though, these approaches are the most relevant methods. But these methods were very complex, time taken, expensive and hazardous chemicals. As a result of these confines, the green chemistry attitudes are remarkably considered to be the most worth protocol in the phyto-synthesis of metal oxide NPs owing to their plenty of rewards such as cost-effectiveness, large-scale commercial production, environment-friendly and pharmaceutical applications [10].

G. superbais a species of flowering plants belonging to Colchicaceae family. It is a perennial, greenish, climbing herb and native to South Africa. Its flower is a state flower of Tamil Nadu and national flower of Tamil Eelam[10]. Since 2000 B.C. itis being used as a traditional medicine by the tribes. Each part of theplant should be used in Siddha, Ayurveda and Unani system of medicine. G. superb a leaf extract is contains many organic components, such assuperbine, colchicine, loriosine, gloriosol, phytosterils and stigmasterin[11].

In the present investigation, Monoethanolamine and G. superba leaf extract capped CeO_2 NPs were prepared through co-precipitation and green method. Synthesized CeO_2 NPs characterized by XRD, FESE, EDAX, UV-Vis and Photoluminescence spectra studies were carried out. From this result, G. superba capped CeO_2 NPs defect level was decreased. In PL results provides strong support for the further development of extensive optical device applications.

II. SYNTHESIS AND CHARACTERIZATION TECHNIQUES

The following high purity chemicals such as Cerium nitrate, Monoethanolamine (MEA), and Sodium hydroxide were used as precursors without further purification.

The MEA added CeO_2 NPs synthesis following, Cerium Nitrate0.1M with capping agent added MEA 0.05M were dissolved double distilled water separate 100ml beaker, than form a homogenous mixture. 0.8M of NaOH was separately dissolved in 100 ml of double distilled water. Then, NaOH solution was added drop wise to the homogenous mixture of Cerium nitrate solution, the pH 12.30 obtained and which yields violet precipitate. The solution with the violet precipitate was stirred at room temperature for 6 h. This solution was refluxed at room temperature for 24 h. Then, a clear solution was obtained, which found to be stable at ambient condition.

The 10 g of G. superba finely cut green leaves were added to 100 mL of double distilled water and boiled at 50-60 °C for 15 min. The obtained extraction was filtered using Whatmann No. 1. Thereafter, 0.1M of Ce $(NO_3)_3 .6H_2O$ salt was added to 100 mL of G. superba leaf extract. This solution was stirred constantly at 80 °C temperature for 6h. A brown precipitate formed and then it was

become a yellowish brown in color on continuous stirring. A schematic diagram of G. superba capped CeO_2 NPs is shown in Fig. 1.Thereafter, the solution was washed several times with double distilled water and ethanol. The precipitate was dried at 120 ˚C. Finally, MEA capped CeO_2 and G. superba capped CeO_2 NP samples were annealed at 700 ºC for 5 h.

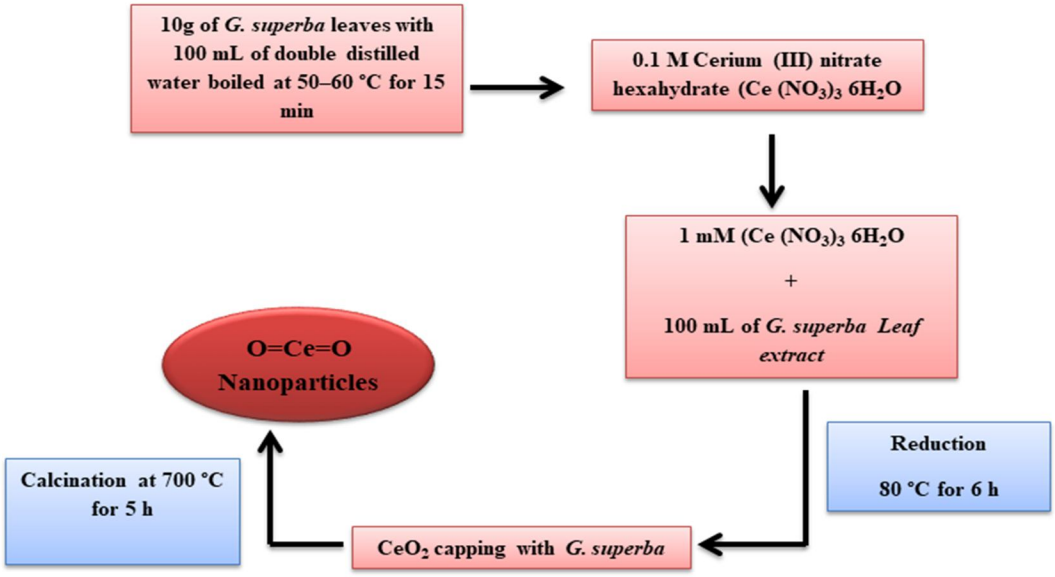

Figure 1. A schematic diagram of G. superba capped CeO_2 NPs

The MEA capped CeO_2 and G. superba capped CeO_2 NPs were characterized by X-ray diffractometer (model: X'PERT PRO PANalytical). The diffraction patterns were recorded in the range of 30º-80º for the MEA capped CeO_2 and G. superba capped CeO_2 NP samples where the monochromatic wavelength of 1.54 Å was used. The samples were analyzed by Field Emission Scanning Electron Microscopy (Carl Zeiss Ultra 55 FESEM) with EDAX (model: Inca). The absorption spectra of MEA capped CeO_2 and G. superba capped CeO_2 NP samples were studied in the range between 200 and 1100 nm by Lambda 35 spectrometer. Photoluminescence spectra were studied using Perkin Elmer-LS 14.

III. RESULTS AND DISCUSSION

A. X-ray diffraction studies

Figure 2 shows the X-ray diffraction pattern of as synthesized MEA and *G.* superba capped CeO_2 NPs. The XRD peaks are at the (2θ) values of (28.58, 33.13, 47.53, 56.38, 59.09, 69.46 and 76.73) and (28.59, 33.12, 47.54, 56.40, 59.1, 69.48, and 76.7) corresponding to (111), (200), (220), (311), (222), (400), (331) and (420) planes of the both MEA and *G. superba*capped CeO_2 NPs respectively, with a space group of $Fm\bar{3}m$ (225). XRD results clearly show reflection peaks are sharp and well crystallized. The lattice parameters CeO_2 NPs is calculated according to the formula

$$\frac{1}{d^2} = \left(\frac{h^2 + k^2 + l^2}{a^2}\right)$$

The lattice constant 'a' value is obtained through the relation a $=\sqrt{d^2(h^2 + k^2 + l^2)}$. The calculated 'a' values are 5.4041 Å and 5.3935 Å for MEA and *G. superba*capped CeO_2 NPs respectively. Changing the capping agent during the synthesis process ofCeO_2NPs, the lattice parameter values and FWHM of the NPs were found to be slightly varied. The average crystallite size of the MEA and *G. superba*capped CeO_2 NPs are calculated by Debye Scherrer's relation

Average crystallite size D = $\frac{k\lambda}{\beta_{Dcos\theta}}$

Where, λ is the wavelength of the radiation (1.54056 Å for CuKα radiation), k is constant which is equal to 0.94, β is the peak width at half-maximum intensity, θ is the peak position. The MEA and G. superba capped CeO_2 NPs average crystallite sizes are calculated at 21.56 nm and 18.71 nm respectively. The crystallite size of G. superba capped CeO_2 NPs decreased as compared to that of MEA capped CeO_2 NPs. The reduction in the crystallite size is mainly due to the many organic components involved in the formation of nanoparticles, which is decreasing the nucleation and subsequent growth rate of the CeO_2 NPs.

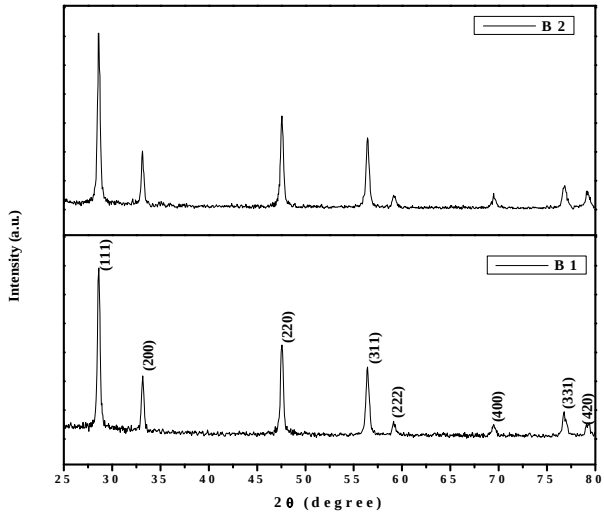

Figure 2. X-ray diffraction pattern of MEA and *G. superba*capped CeO_2 NPs.

B. Morphological and Elemental composition of CeO_2

Figure 3 (a-b) shows the topographical analysis of as-synthesized MEA and G. superba capped CeO_2 NPs. From the FESEM image, the synthesized MEA and G. superba capped CeO_2 NPs are exhibit cubic structure. The average particle size observed at 35 and 27 nm for both CeO_2NPs respectively. G. superba leaf capped CeO_2 NPs possess decreased as compared to that of chemical synthesized MEA capped CeO_2 NPs. This size reduction may be presence of various organic components involved in the NPs formation. Metal element composition of CeO_2 NPs as shown in Fig. 3(c-d). From EDAX results, the Ce and O atomic percentage are observed at (31.13 % & 68.87%) and (73.62 % & 26.38%) for MEA capped CeO_2 and G. superba capped CeO_2 NPs respectively. The G. superba capped CeO_2 NPs oxygen percentage increase with decrease the cerium percentage as compared to that of MEA capped CeO_2 NPs, which may be NPs formed using G. superba plant extract.

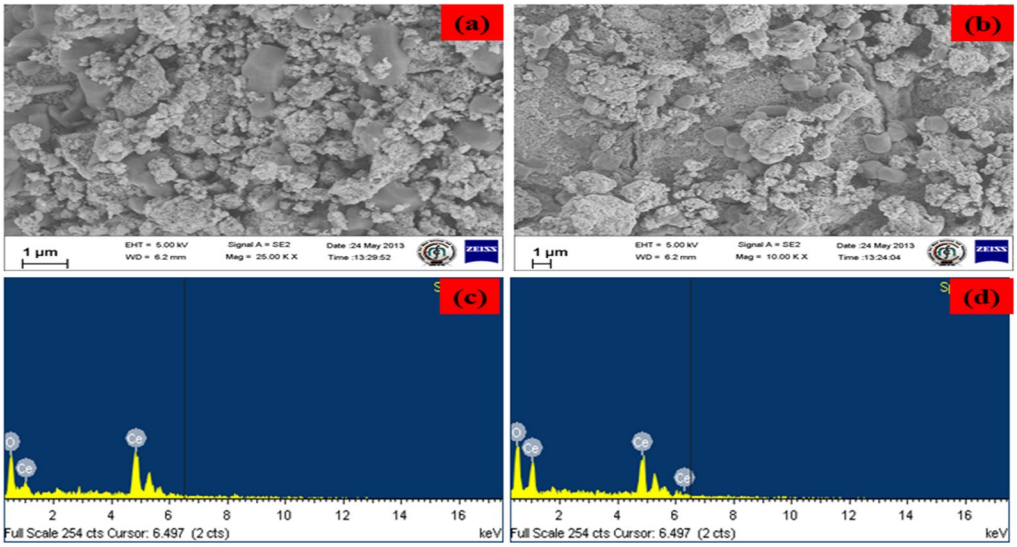

Figure 3 (a-b). FESEM image of MEA and G. superba capped CeO_2 NPs and (c-d) EDAX spectra of MEA and G. superba capped CeO_2 NPs.

C. Ft-ir Spectroscopic Studies

FT-IR spectrum of MEA and *G.* superbacapped CeO_2 NPs shown in Fig. 4. The broad absorption O-H peak observed at 3750-3000 cm^{-1} [12] From the FTIR spectra, the O-H stretching of residual alcohols, water and Ce-OH found for 3422 and 3442 cm^{-1} for MEA and G. superba capped CeO_2 NPs respectively. The C-H vibration characteristic bands are observed at 2939 and 2911 cm^{-1} for CeO_2

NPs [13] Absorption band at 1641 cm^{-1} is ascribed O-H symmetric stretching for MEA capped CeO_2 NPs [13]. The Ce-O-Ce stretching frequency are found to be 1008 and 1044 cm^{-1} for MEA and G. superba capped CeO_2 NPs respectively. The Ce-O-C bending mode vibration is observed at 687 and 682 cm^{-1} for both CeO_2 NPs [14,15]. From the FT-IR results, the strong Ce-O stretching vibrations is centered at 505 and 508 cm^{-1} for MEA and G. superb a capped CeO_2 NPs respectively.

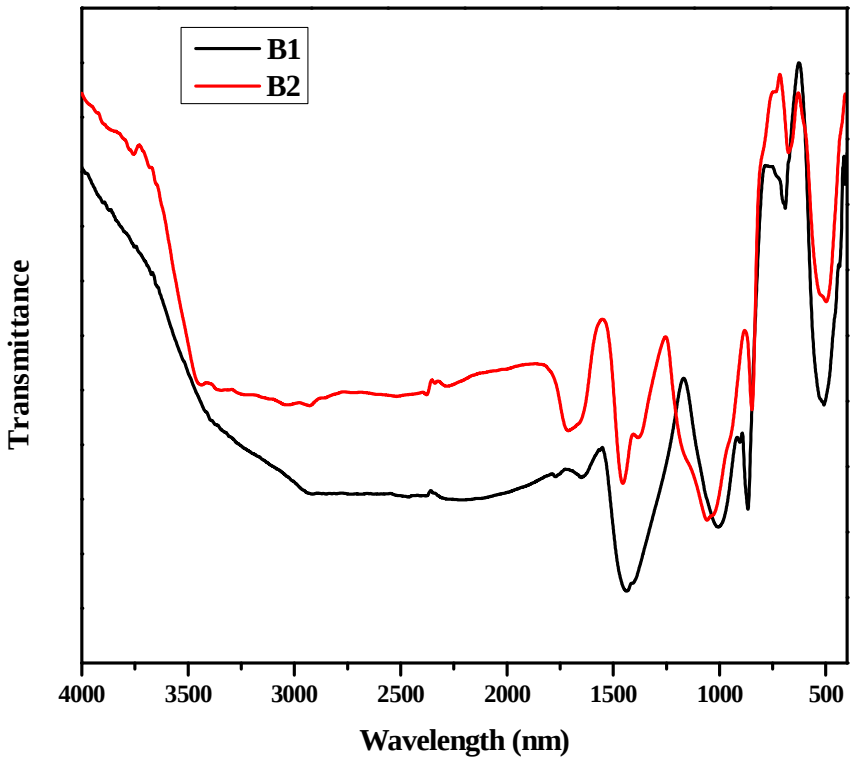

Figure 4. FT-IR spectra of MEA and G. superba capped CeO_2 NPs.

D. UV-Vis Spectroscopic Studies

Figure 5 shows the UV-Vis absorption spectrum of MEA and G. superba capped CeO_2 NPs. From the UV-Vis results, the absorption edge peaks are located at 317 and 313 nm for MEA and G. superba capped CeO_2 NPs, due to the photo excitation of electrons from the valence band to the conduction band. The absorption edge peak red shift is observed for MEA capped CeO_2 NPs as compared to that of G. superba capped CeO_2 NPs. This impact, the reduction of CeO_2 band gaps caused by the G. superba capping effect. The band gap is calculated using tauc relation [16].Considering direct band transition in CeO_2 NPs, a plot between $(\alpha h\upsilon)^2$Vs. hυ and extrapolating the linear portion of the absorption edge to find the intercept with energy axis is shown in Fig. 5 (a-b). Calculated band gaps of MEA and G. superbacapped CeO_2 NPs values are found to be 2.6 eV and 2.95 eV respectively. The band gap ofG. superba capped CeO_2NPs possess more than that of MEA capped CeO_2 NPs, increasing the band gap may be due to the many organic components involved in the formation of nanoparticles. This result obey the quantum confinement effect shows the particles are in few nanometer level [10].

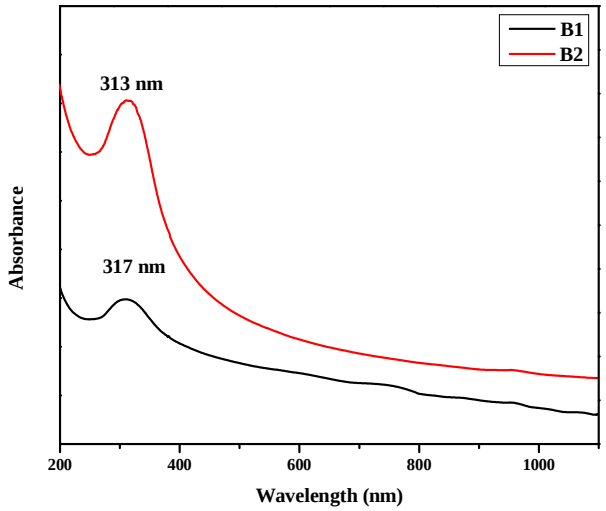

Figure 4. UV-Visible spectra of the MEA and G. superba capped CeO_2 NPs.

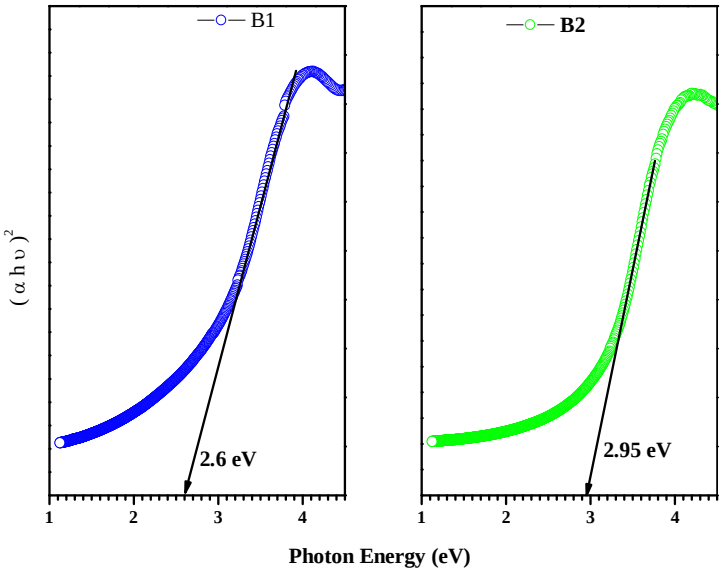

Figure 5 Band gaps of MEA and G. superba capped CeO_2 NPs.

E.Photoluminescence spectroscopic studies

The room temperature photoluminescence emission spectra of MEA and G. superbacapped CeO_2 NPs are shown in Fig. 6(a-b). The synthesizedMEA and G. superba capped CeO_2 NPs were observed in the excited wavelength 325 nm. The PL emission wavelength is observed at (366 nm, 387 nm, 400 nm, 458 nm and 489 nm) and (389 nm, 414 nm, 439 nm, 457 and 482 nm) for MEA and G. superba capped CeO_2 NPs respectively. In case of MEA capped CeO_2 NPs, the two UV emission peaks observed at 366 nm and 387 nm are corresponding to the near band edge (NBE) emission, this is due to the recombination of free exactions[17]. The violet emission center at 400 nm, which is due to the charge transitions from the 4f band to the valence band of CeO_2 [18]. Blue emission observed at 458 nmisattributed to the localization of the energy levels among the Ce 4f and O2p bands. The blue-green emission centered at 485 nm, is described to surface defects. Blue shift observed for G. superba capped CeO_2 NPs emission values (389 nm, 414 nm, 439 nm, 457 and 482 nm) as compared to that of MEA capped CeO_2 NPs. This may occur from different origins, such as

electron phonon coupling, lattice distortion, localization of charge carriers due to interface effects and point defects. In PL spectra the defect level emission was reduced G. superba capped CeO_2 NPs. The optoelectronic properties mainly depend on the reduction of defect level in material, which influenced by electron phonon coupling interaction. In the present investigation, G. superba capped CeO_2 NPs defect level was decreased. In PL results provides strong support for the further development of extensive optical device applications.

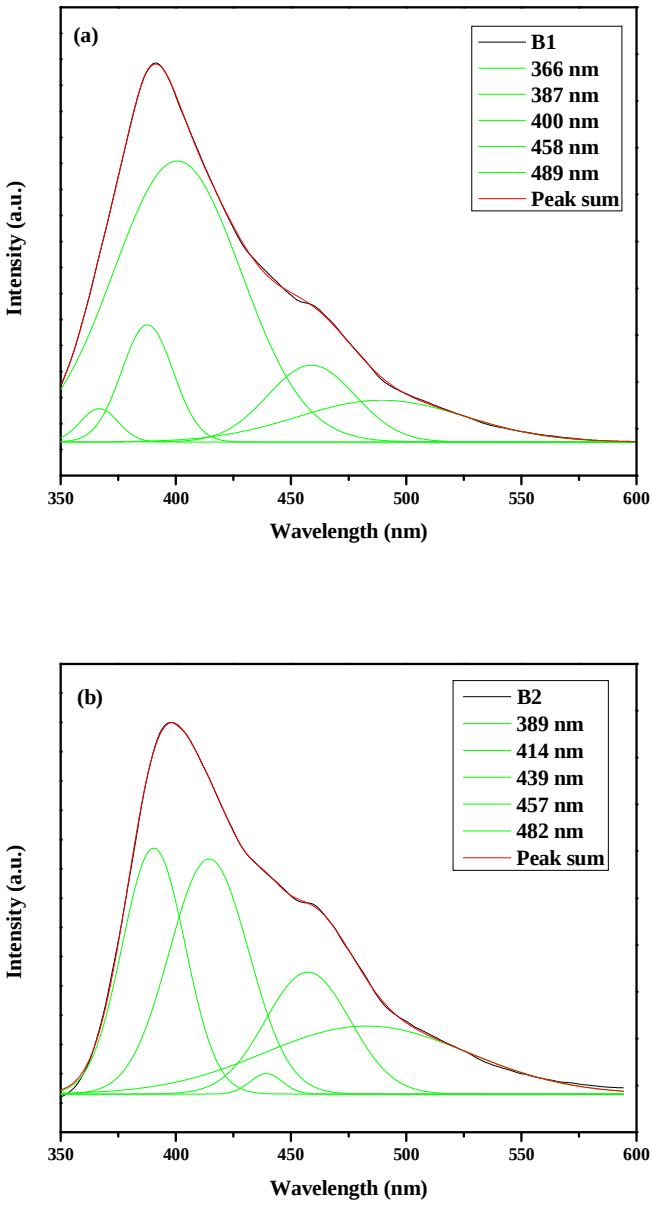

Figure 6 Photoluminescence spectra of MEA and G. superba capped CeO_2 NPs.

IV. CONCLUSIONS

In summary, the CeO_2 NPs were synthesized by co-precipitation and green method. Synthesized MEA and G. superba capped CeO_2 NPs were exhibited cubic phase, identified by X-ray diffraction studies. In the FESEM image, the both CeO_2 NPs were formed cubic structure. The Ce and O elemental composition were identified using EDAX spectra. Vibrational functional groups were identified using FT-IR spectra. From the UV-Vis studies, the absorption peaks edges were observed at 317 and 313 nm for both CeO_2 NPs respectively. In PL emission spectra the defect level emission was reduced G. superba capped CeO_2 NPs as compared to

the MEA capped CeO_2 NPs. The optoelectronic properties mainly depends on reduction of defect level in material, which influenced by electron phonon coupling interaction. In the present investigation, G. superba capped CeO_2 NPs defect level was decreased. In PL results provides strong support for the further development of extensive optical device applications.

REFERENCES

[1] F.P.Go, A. E. Saatci, O. Orhan, B.Keskin, K.Kutlu, Structural, optical and electrochromic properties of cerium dioxide thin films prepared by sol-gel dip coating method. Materials Science in Semiconductor Processing. 38:300-5, 2015.
[2] V. Ramasamy, G.Vijayalakshmi, Effect of Zn doping on structural, optical and thermal properties of CeO_2 nanoparticles. Superlattices and Microstructures.85:510-21, 2015
[3] A. Masalov, O. Viagin, P.Maksimchuk,V. Seminko,I.Bespalova,A. Aslanov,Y. Malyukin,Zorenko, Formation of luminescent centers in CeO_2nanocrystals. Journal of luminescence. 145:61-4 2014
[4] F. Zhang, S. W. Chan, J. E. Spanier,E. Apak,Q. Jin,R. D. Robinson, I. P. Herman, Cerium oxide nanoparticles: size-selective formation and structure analysis. Applied physics letters. 80(1):127-9, 2002
[5] J.D. Hu,Y. X. Li,X. Z. Zhou, M.X. Cai, Preparation and characterization of ceria nanoparticles using crystalline hydrate cerium propionate as precursor. Materials Letters. 61(28):4989-92, 2007
[6] H. Wang,J. J. Zhu, J. M. Zhu,X. H. Liao, S. Xu,T. Ding,H. Y. Chen, Preparation of nanocrystalline ceria particles by sonochemical and microwave assisted heating methods. Physical Chemistry Chemical Physics.4(15):3794-9, 2002
[7] X. H. Liao,J. M. Zhu,J. J. Zhu,J. Z. Xu,H. Y. Chen, Preparation of monodispersednanocrystalline CeO2 powders by microwave irradiation. Chemical Communications. (10):937-8, 2001.
[8] F. Czerwinski,J. A. Szpunar, The nanocrystalline ceria sol-gel coatings for high temperature applications. Journal of Sol-Gel Science and Technology. 9(1):103-14, 1997
[9] S. Y. Yao,Z. H. Xie,Deagglomeration treatment in the synthesis of doped-ceria nanoparticles via coprecipitation route. Journal of materials processing technology. 186(1):54-9, 2007.
[10] A. Arumugam, C.Karthikeyan, A. S.Hameed, K.Gopinath, S. Gowri, V. Karthika, Synthesis of cerium oxide nanoparticles using Gloriosasuperba L. leaf extract and their structural, optical and antibacterial properties. Materials Science and Engineering: C. 49:408-15, 2015
[11] S. Jana, G. S.Shekhawat, Critical review on medicinally potent plant species: Gloriosasuperba. Fitoterapia.82(3):293-301, 2011
[12] B. Choudhury,P. Chetri,A. Choudhury, Annealing temperature and oxygen-vacancy-dependent variation of lattice strain, band gap and luminescence properties of CeO_2 nanoparticles. Journal of Experimental Nanoscience. 10(2):103-14, 2015
[13] R. Murugan, G. Ravi, G. Vijayaprasath, S. Rajendran, M. Thaiyan, M. Nallappan, M. Gopalan, and Y. Hayakawa, Ni–CeO_2 spherical nanostructures for magnetic and electrochemical supercapacitor applications. Physical Chemistry Chemical Physics, 19(6),4396-4404, 2017.
[14] M. G. Sujana,K. K. Chattopadyay,S. Anand, Characterization and optical properties of nano-ceria synthesized by surfactant-mediated precipitation technique in mixed solvent system. Applied Surface Science. 254(22):7405-9, 2008.
[15] G. dos Santos, A. J. Simmonds, H. M. Krause, A stem-loop structure in the wingless transcript defines a consensus motif for apical RNA transport. Development. 135(1):133-43, 2008.
[16] L. Xiao-Bo, S. Hong-Lie, Z.Hui, L. Bin-bin, Optical properties of nanosizedZnO films prepared by sol-gel process. Trans. Nonferrous Met. Soc. China., 17, 3814-3817 (2007).
[17] L. Wang, J. Ren, X. Liu, G. Lu, Y. Wang, Evolution of SnO_2 nanoparticles into 3D nanoflowers through crystal growth in aqueous solution and its optical properties. Materials Chemistry and Physics. 127(1):114-9, 2011.
[18] R. Murugan, G.Vijayaprasath, T. Mahalingam, G.Ravi, Enhancement of room temperature ferromagnetic behavior of rf sputtered Ni-CeO_2 thin films. Applied Surface Science, 390, 583-590 (2016).

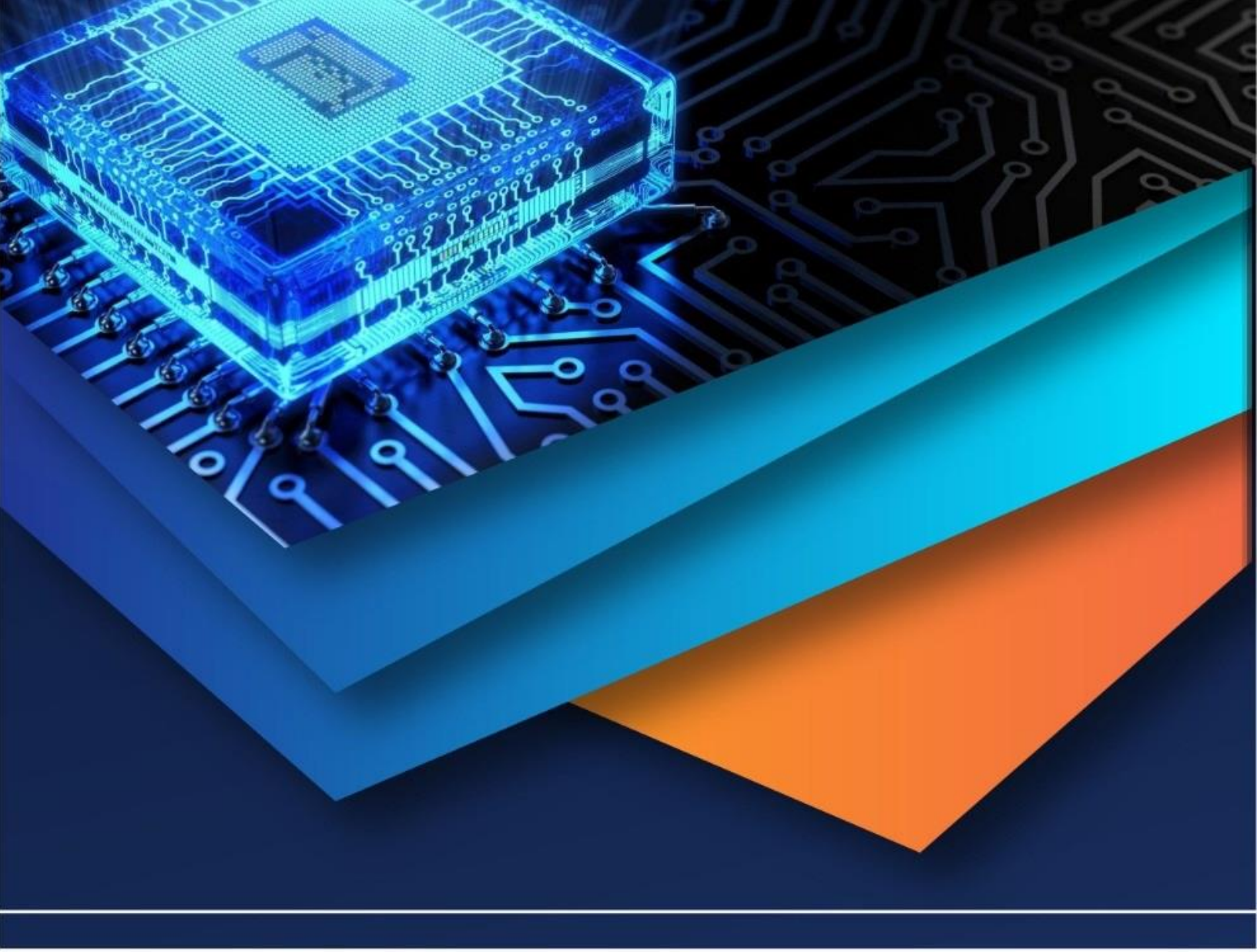

10.22214/IJRASET

45.98

IMPACT FACTOR: 7.129

IMPACT FACTOR: 7.429

INTERNATIONAL JOURNAL FOR RESEARCH

IN APPLIED SCIENCE & ENGINEERING TECHNOLOGY